

# MICROBIOME OF GRAND CANYON CAVERNS, A DRY SULFURIC KARST CAVE IN ARIZONA, SUPPORTS DIVERSE EXTREMOPHILIC BACTERIAL AND ARCHAEOAL COMMUNITIES

Raymond Keeler<sup>1</sup> and Bradley Lusk<sup>2,C</sup>

---

## Abstract

We analyzed the microbial community of multicolored speleosol deposits found in Grand Canyon Caverns, a dry sulfuric karst cave in northwest Arizona, USA. Underground cave and karst systems harbor a great range of microbial diversity; however, the inhabitants of dry sulfuric karst caves, including extremophiles, remain poorly understood. Understanding the microbial communities inhabiting cave and karst systems is essential to provide information on the multidirectional feedback between biology and geology, to elucidate the role of microbial biogeochemical processes on cave formation, and potentially aid in the development of biotechnology and pharmaceuticals. Based on the V4 region of the 16S rRNA gene, the microbial community was determined to consist of 2207 operational taxonomic units (OTUs) using species-level annotations, representing 55 phyla. The five most abundant Bacteria were *Actinobacteria*  $51.3 \pm 35.4$  %, *Proteobacteria*  $12.6 \pm 9.5$  %, *Firmicutes*  $9.8 \pm 7.3$  %, *Bacteroidetes*  $8.3 \pm 5.9$  %, and *Cyanobacteria*  $7.1 \pm 7.3$  %. The relative abundance of Archaea represented  $1.1 \pm 0.9$  % of all samples and  $0.2 \pm 0.04$  % of samples were unassigned. Elemental analysis found that the composition of the rock varied by sample and that calcium ( $6200 \pm 3494$  ppm), iron ( $1141 \pm 1066$  ppm), magnesium ( $25 \pm 17$  ppm), and phosphorous ( $37 \pm 33$  ppm) were the most prevalent elements detected across all samples. Furthermore, carbon, hydrogen, and nitrogen were found to compose  $4.7 \pm 4.9$  %,  $0.3 \pm 0.4$  %, and  $0.1 \pm 0.1$  % of samples, respectively. Finally, Raman spectra compared to the RRUFF Project database using CrystalSleuth found that the mineral composition of the speleosol consisted of calcite, hematite, paraspurrite, quartz, and trantnerite. These data suggest that dry sulfuric karst caves can harbor robust microbial communities under oligotrophic, endolithic, and troglomorphic conditions.

---

## INTRODUCTION

Microorganisms are the principle components of the formation of the Earth's atmosphere, hydrosphere, and surface, and play a central role in karst cave formation and the cycling of organic and inorganic nutrients. For example, hydrogen sulfide-producing microbes can contribute to the formation of sulfuric karst caves in aqueous environments in a process called sulfuric acid speleogenesis (Engel et al., 2004). During sulfuric acid speleogenesis, limestone dissolves and hypogenic karst emerges as a result of artesian flow (Klimchouk et al., 2000). (An overview of this process is provided in Equations S1–S3.) As the limestone loses mass, microbial and chemical processes collectively drive a pedogenic erosion process that forms a bedrock-facing punk rock layer (Hill, 1987) and a cave-passage-facing oxide layer (Spilde et al., 2006). This process results in the formation of corrosion residues, or ferromanganese deposits (FMD), called speleosol (Spilde et al., 2009). The iron and manganese-rich composition of the oxide layers in speleosol is the result of microbial interactions with the minerals at the interface of the bedrock, punk rock, and oxide layer (Spilde et al., 2006; 2009).

Extremophiles are microorganisms that survive under conditions that are inhospitable to most life on Earth and are expected to be discovered in dry sulfuric karst caves given that the conditions are oligotrophic (limited access to essential nutrients), endolithic (ability to grow within rock or mineral pores) (Wierzchos et al., 2011), xerophilic (limited access to water) (Forbes, 1998; Lebre et al., 2017), and troglomorphic (ability to grow within caves). Elucidating microbial life inhabiting extremophilic subterranean zones, including cave and karst systems, has many benefits. For example, it expands our concept of hospitable zones when searching for astrobiological life on other planets (Northup et al., 2011; Wierzchos et al., 2011; Lusk et al., 2019a). Next, the discovery of new microorganisms and genes from caves has led to the development of antibiotics and antifungals that may suppress the spread of diseases, including white-nose syndrome (WNS) in bats (Blehert et al., 2009; Hamm et al., 2017). Lastly, finding microbes that interact with metals and ores will assist in the discovery of biocatalysts, which can be used to interface living cells with materials for the production of biotechnology, including microbial electrochemical cells (Eddie et al., 2016; Lusk et al., 2018a; Sun et al., 2018).

Understanding the fundamental interactions of abiotic materials with biotic life, including microorganisms that are able to reduce and oxidize materials to produce or dissolve solid metals and ores, will enhance our understanding of the biogeochemical processes that shape the Earth (Eddie et al., 2016; Lusk et al., 2018a; 2019a; Sun et al., 2018). Spe-

---

<sup>1</sup>Central Arizona Grotto of the National Speleological Society, Phoenix, AZ, United States of America.

<sup>2</sup>ScienceTheEarth, Mesa, AZ, United States of America.

<sup>C</sup>Corresponding author: ScienceTheEarth@gmail.com, ORCID: 0000-0002-3094-805X.

leiosols in caves, for example, provide an ideal habitat for investigating robust microbial communities associated with geomicrobially-mediated sulfuric acid speleogenesis. Given the variety of regions and conditions in which geomicrobially-mediated sulfuric acid speleogenesis occurs (Engel et al., 2004), a robust and systematic study of microorganisms residing in caves is essential to develop a comprehensive explanation of this phenomenon.

Grand Canyon Caverns (GCC) is a commercial dry cave in northwest Arizona, USA that was formed via sulfuric acid speleogenesis. In February 2013, approximately 100 meters of steeply up-trending new passages and rooms were discovered containing multicolored corrosion residues composed of punk rock (Hill, 1987) and containing an oxide layer, also called speleosol (Spilde et al., 2006; 2009). Similar deposits in Lechuguilla and Spider Caves located in the Guadalupe Mountains of New Mexico were previously observed to harbor microbial life (Northup et al., 2003; Spilde et al., 2006). The formations discovered in GCC were kept isolated from tourists for the purpose of conducting research on their microbial inhabitants. To assess the diversity of microorganisms, 14 dry samples from three separate areas were collected from sections throughout the cave that had minimal perturbation from human activity (sampling locations shown in Fig. 1). Samples were analyzed for their elemental, mineralogical, and microbial composition.

## MATERIALS AND METHODS

### Cave Description and Overview

GCC is a commercial dry sulfuric karst cave in northwest Arizona, USA (35°31'41.9" N 113°13'52.7" W) that is located about 100 kilometers south of the southern rim of Grand Canyon National Park. The cave is positioned in the upper part of the Redwall limestone from the Late Devonian / Early Mississippian periods (Huddle and Dobrovlny, 1952) with a small, inactive volcano located five kilometers northwest. The Redwall limestone dates back to approximately 350 Ma and is composed of 99.5 % pure limestone (Gootee, 2014; 2019). During this period, the region was part of a shallow tropical sea in the equatorial continent of Laurentia (Price, 1999; Gootee, 2019). Presently, the cave has no known freestanding bodies of water and has an average relative humidity of 79.5 % and temperature of 15 °C. There are no indications of the presence of non-microbial life in the cave; however, there have not been surveys for non-microbial life in GCC.

A map of the cave, including sample collection locations, is shown in Figure 1. Annually, thousands of tourists visit GCC. At the time of sample collection, cave tours were limited to the main sections of GCC including the Chapel of Angels, the Halls of Gold, Snowball Palace, and the Mystery Chamber, and ceased at gates 1 and 2. Gates 1 and 2 were installed to limit access to newly-discovered areas of the cave for the purpose of mapping and conducting research. Due to the observation of multicolored speleosol deposits on the cave walls on top of the underlying limestone (Fig. 2), 14 samples were collected from Sugar Hill, below the ropes to Disappointment Dome, and Disappointment Dome. Since collecting samples, tourism has now extended to Sugar Hill and below the ropes to Disappointment Dome.

### Sample Collection

Sterile Falcon tubes (15 mL) were used to store 14 samples (~500 mg each) that were collected in the cave. Each sample was collected by scraping the Falcon tube directly against the cave surface to collect solid surface deposits of

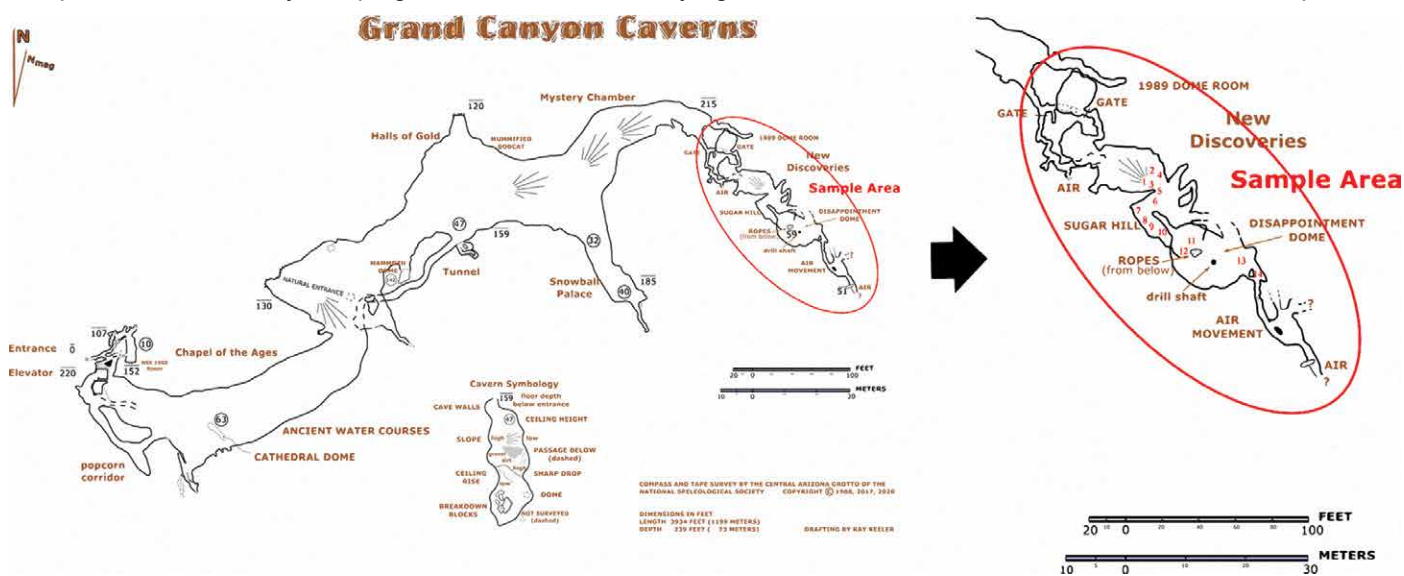


Figure 1: Cave map for Grand Canyon Caverns. Inset on right shows collection locations for 14 samples. The three major sampling locations were Sugar Hill, below the ropes to Disappointment Dome, and Disappointment Dome. At the time of collection, active tourism in the cave ceased at gates 1 and 2.

speleosol from the cave walls. After placing the lid on the Falcon tube, each tube was wrapped in aluminum foil, placed on icepacks, stored in an ice chest, and transported to a  $-80^{\circ}\text{C}$  freezer. All samples were collected in the deep zone of the cave, at least 200 m from the nearest entrance with no surface visible light. Sample collection locations varied from a meter to several meters apart and are shown in the inset to Figure 1.

### Sample Identification via Raman Spectroscopy and CrystalSleuth

The mineral composition of each rock sample was identified using a Renishaw via Reflex Micro-Raman confocal Raman Microscope (Renishaw, West Dundee, Ill., U.S.A.) equipped with a Leica 566066 N PLAN EPI 20X/0.4 (Leica, Wetzlar, Germany) objective lens and two laser excitation sources: a near infrared diode laser source (300 mW) with an excitation wavelength of 785 nm and an Argon ion laser source (25 mW) with an excitation wavelength of 514 nm. For spectra captured at 785 nm, laser power was varied from 1–50 %, exposure time set to 1–3 seconds, and spectra were averaged over five accumulations. For spectra captured at 514 nm, laser power was set to 100 %, exposure time set to one second, and spectra were averaged over twelve accumulations. For each sample, spectra at 785 nm and 514 nm were taken

at three different locations. After acquiring Raman spectra, light images were acquired under white light using the same objective lens. Spectra were compared to the RRUF Project database using the CrystalSleuth Application Version: May 19, 2008 (Laetsch and Downs, 2006). For identifying samples, background was subtracted, cosmic ray events (CRE) were removed, and a cutoff of 90 % similarity was used to determine a match. Filtered spectra with corresponding light images can be found in Figure S2 GCC1-14.

### Digestion and Quantification of Elements

Samples were digested ( $255.3 \pm 6.2$  mg) using a MARS 5 Microwave Digester (CEM Corporation, Matthews, N.C., U.S.A.). For the microwave process, each sample was weighed and 10

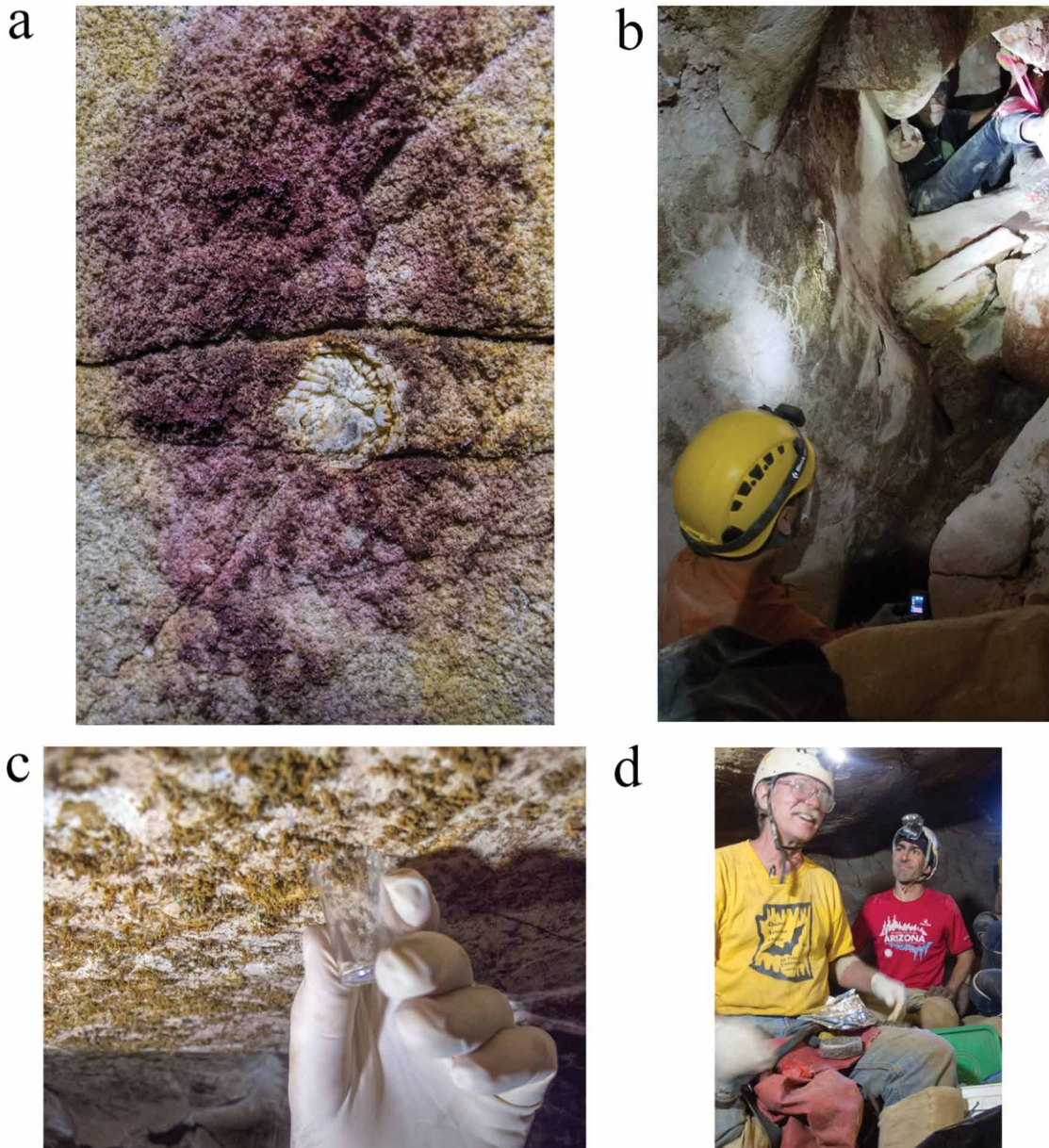


Figure 2: a) Multicolored, powdery speleosol deposit on the cave wall surrounding a Late Devonian/ Early Mississippian period rugose coral fossil (photo credit: Paul Jorgenson). b) Brown colored powdery speleosol deposit on cave wall with cavers shown for scale. c) Collecting a sample from a yellow colored speleosol deposit (photo credit: Paul Jorgenson). d) Co-authors Raymond Keeler and Bradley Lusk wrapping samples in foil and collecting video documentation of cave expedition (photo credit: Paul Jorgenson).

mL of concentrated trace metal grade nitric acid was added. All sample tubes were heated to 180 °C in 5 minutes and held at 180 °C for 10 minutes in a 1600 W microwave. After heating, samples were cooled for 5 minutes. The elemental composition of samples was analyzed using a Thermo iCap 6300 inductively coupled plasma optical emission spectrometer (ICP-OES) (Thermo Fisher Scientific, Waltham, Mass., U.S.A.) with a duo plasma source. Samples were diluted at 1:10 with nano-pure water to acquire accurate measurements for the following metals: Ag, Al, As, B, Ba, Be, Bi, Cd, Co, Cr, Cu, K, Li, Mg, Mn, Mo, Na, Ni, P, Pb, S, Sb, Se, Si, Sr, Ti, V, and Zn. Due to the high concentration of Ca and Fe, separate samples for these elements were diluted at 1:1000 with nano-pure water. Sample 5 did not contain enough mass for analysis using the ICP-OES.

For quantification of total C, H, and N, a Perkin Elmer PE 2400 Elemental Analyzer was used with  $5.4 \pm 0.6$  mg per sample (<https://cores.research.asu.edu/metals-environmental-and-terrestrial-analytical-laboratory/equipment/analytical-chn-elemental>). Samples were flash combusted at 1760 °C. Resulting gases were chemically scrubbed of the halogens (and of sulfur in the CHN mode) and were separated in a GC column. Detection was conducted by a thermal conductivity detector (TCD).

### Scanning Electron Microscopy (SEM) and Color Images

Approximately 5 mg from each of the 14 samples was fixed with 4 % glutaraldehyde for 12 h at 4 °C and then washed and stored in 10 mM PBS (pH 7) solution for ~1 h. Next, the samples were treated with 1% osmium tetroxide for 15 min, followed by graded ethanol series dehydration (50%, 70%, 95%, and 100% for 5 min each), then critical point dried, and ultimately mounted on an aluminum stub. Samples were sputter-coated with Au/Pd alloy with a Technics Hummer II sputter coater. Imaging was conducted using a JEOL JSM6300 SEM at 15X – 95kX with an accelerating voltage of 15 kV. Color images of samples (Fig. 3) were taken with a Samsung Galaxy S7 under white light conditions.

### DNA Extraction and Library Preparation for 16S rRNA Sequencing

DNA from the 14 samples was extracted using the PowerSoil DNA Isolation Kit (MO BIO, Carlsbad, Calif., U.S.A.) per the manufacturer's manual. DNA was released from cells via bead beating using PowerBead tubes (MO BIO, Carlsbad, Calif., U.S.A.). Amplicon sequencing of the V4 region of the 16S rRNA gene was performed with the barcoded primer set 515f/806r designed by Caporaso et al. (2012), following the protocol proposed by the Earth Microbiome Project (EMP <https://earthmicrobiome.org/protocols-and-standards/16s/>) for the library preparation. PCR amplifications for each sample were done in triplicate, then pooled and quantified by using Quant-iT PicoGreen dsDNA Assay Kit (Invitrogen, ThermoFisher Scientific, Waltham, Mass., U.S.A.). A total of 240 ng of DNA per sample was pooled and then cleaned using QIA quick PCR purification kit (QIAGEN, Valencia, CA, USA). The PCR pool was quantified by Illumina Library Quantification Kit ABI Prism (Kapa Biosystems, Wilmington, MA, USA). The DNA pool was determined and diluted to a final concentration of 4 nM, then denatured and diluted to a final concentration of 4 pM with 30 % PhiX. Finally, the DNA library was loaded in the MiSeq Illumina Sequencer (Illumina, San Diego, CA, USA) using the chemistry version 2 (2 × 150 paired-end) and following manufacturer directions. All samples were sequenced in the Microbiome Analysis Laboratory at Arizona State University (Tempe, Ariz., U.S.A.).

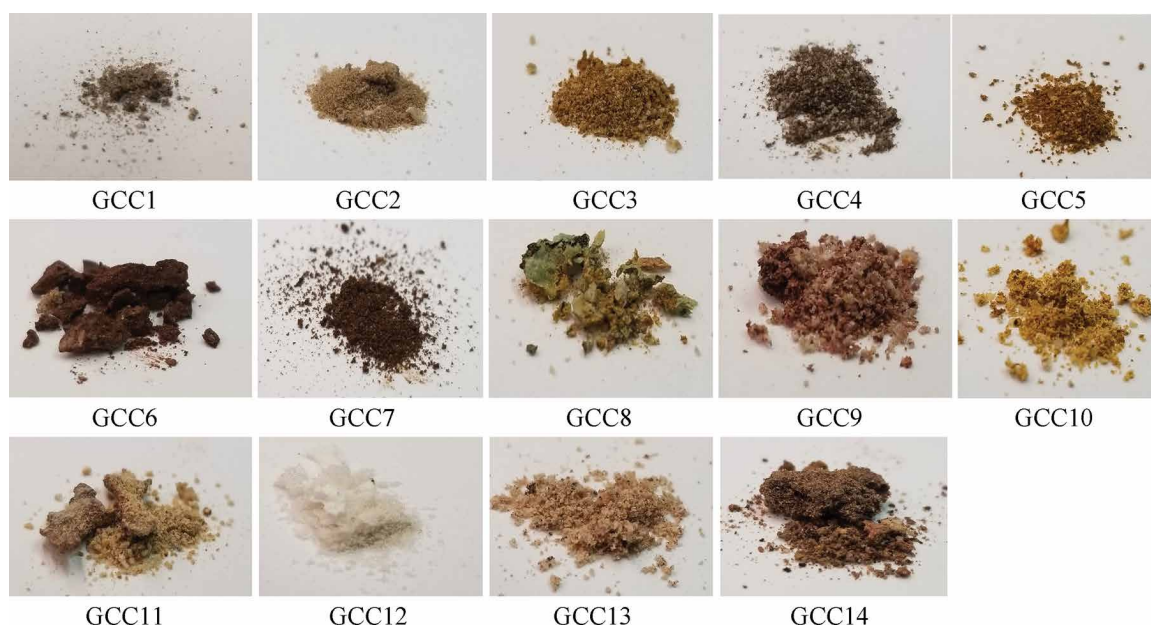


Figure 3: Macroscopic images of samples 1–14.

### Determination of Microbial Taxonomy

The analysis of the 16S rRNA gene sequences was performed using the Quantitative Insights into Microbial Ecology 2 software package (QIIME2, version 2018.4) (Bolyen et al., 2019). Sequences were open reference clustered into Operational Taxonomic Units (OTUs) against the Silva-132

database (Quast et al., 2013) using an identity threshold of 97 % with the vsearch algorithm (Rideout et al., 2014). After the alignment of the sequences, the OTU table was constructed and then filtered for the removal of singletons, and chimeras and borderline chimeras using vsearch uchime-denovo (Edgar et al., 2011). Eukaryotic homologues were also removed. The OTU table was rarefied to the minimum number of sequences obtained among the samples (GCC 12 with 44,297 sequences) and an alpha diversity rarefaction table was constructed using 10 iterations for each sample data point. Finally, the taxonomy was assigned to OTUs using a Scikit-learn naïve-Bayes taxonomy classifier against the Silva\_132\_97\_16s OTUs reference sequences (Pedregosa et al., 2018), with counts for classified OTUs at all phylogenetic levels (Table S1), and an Excel file with all observed OTUs (Table S2).

## RESULTS AND DISCUSSION

This research study assesses the mineralogical and microbial diversity of multicolored speleol deposits found in GCC. These deposits ranged from several centimeters to several meters spanning entire walls of the cave. Similar formations have been observed in Lechuguilla and Spider Caves in New Mexico, United States (Northup et al., 2003), the Cave of Altamira in Spain (Jurado et al., 2007), Roraima Sur Cave in Venezuela (Barton et al., 2014), and Asperge Cave in France (Tisato et al., 2015), Figure 2a-d shows examples of formations from which samples were collected and the acquisition of samples within the cave. As shown in Figure 2a, some multicolored formations were found surrounding fossils of rugose coral from the Late Devonian / Early Mississippian period (Huddle and Dobrovlny, 1952; Pedder and Murphy, 2004; Denayer et al., 2012). Figure 2b shows a deposit spanning approximately three meters of a wall with surveying cavers to add scale. Figure 2c shows sample collection directly from the cave walls and Figure 2d shows cavers wrapping samples into foil and documenting the sample locations.

Speleol samples collected at 14 sites in the cave varied in color and consistency (Fig. 3). Raman spectroscopy was used to determine the mineral contents of each sample (Table 1) by comparing spectra to the RRUFF™ Project database using the CrystalSleuth Application Version: May 19, 2008 (Laetsch and Downs, 2006). The samples were primarily composed of calcite, hematite, paraspurrite, quartz, and trattnerite. A detailed description of each sample can be found in the supplemental information and filtered spectra with light microscopy images in Figure S2 GCC1-14.

An elemental analysis was done on GCC samples (Tables 2a-b). The composition of the speleol deposits varied by sample with calcium (6200 ± 3494 ppm), iron (1141 ± 1066 ppm), magnesium (25 ± 17 ppm), and phosphorous (37 ± 33 ppm) the most prevalent elements detected.

**Table 1. Identity of compounds observed within samples collected from 14 collection sites in Grand Canyon Caverns as revealed by comparing Raman spectra collected using either a 514 nm or 785 nm laser source to the RRUFF Project database. Only spectra which shared at least 90 % similarity are shown with the exception of Sample 9, as indicated by []. The \* indicates that no match values higher than 90 % were observed under this condition. Order of percentages coincides with the order of RRUFF ID.**

Sample	Wavelength = 514 nm		Wavelength = 785 nm	
	Compound	% Match	Compound	% Match
GCC 1	Calcite	99, 98, 97	Calcite	92
GCC 2	Calcite	99, 98	Calcite, Paraspurrite	94, 90, 93
GCC 3	Calcite	98	*	*
GCC 4	Calcite	97, 95	*	*
GCC 5	Calcite	99	Calcite	96
GCC 6	Quartz	99, 99	Trattnerite	91, 90
GCC 7	Quartz	99	*	*
GCC 8	Calcite	97	*	*
GCC 9	Gypsum	[85]	*	*
GCC 10	Calcite	96	*	*
GCC 11	Calcite	96, 93	*	*
GCC 12	Calcite	98, 98, 95	Calcite	98, 95
GCC 13	Calcite	96, 94	Paraspurrite, Calcite	92, 91
GCC 14	Hematite	92	*	*

ed across all samples. Aluminum ( $49 \pm 57$  ppm) was observed in seven samples, manganese ( $43 \pm 58$  ppm) in 12 samples, potassium ( $93 \pm 88$  ppm) in 13 samples, and silicon ( $5 \pm 2$ ), sodium ( $5 \pm 5$ ), and zinc ( $23 \pm 62$ ) in all samples. Total carbon, hydrogen, and nitrogen made up  $4.7 \pm 4.9\%$ ,  $0.3 \pm 0.4\%$ , and  $0.1 \pm 0.1\%$  of samples, respectively (Table 3).

Due to the mixed nature of each sample, it is possible that minerals present in small quantities are difficult to observe using Raman spectroscopy since they are masked by more ubiquitous compounds. Nevertheless, the prevalence of Ca, C, Fe, Mg, Na, P, Si, and Zn are likely the result of the hematite, paraspurrite, trantnerite, and limestone that contributes to the composition of the punk rock and underlying cave walls. The high Fe content likely is due to the accumulation of iron oxides resulting from microbial-induced enrichment in the oxide layer of the speleosol (Spilde et al., 2009), although auto-oxidation of ferrous iron at neutral pH may also play a role (Emerson and Moyer, 1997). The presence of Al, Ca, Fe, K, Mg, Mn, and Si corroborates previous literature documenting microbial interactions with minerals in ferromanganese deposits (FMD), or speleosol, including todorokite, lepidocrocite, goethite, illite, and hematite (Northup et al., 2003; Spilde et al., 2005).

Scanning electron microscopy (SEM) on each of the samples (Fig. 4) revealed the presence of diverse microbial morphologies associated with the speleosol. Diverse biological communities have also been observed and associated with cave mineralogy in other cave sites (Cunningham et al., 1995; Boston et al., 2009; Dhami et al., 2018). Although SEM cannot be used to identify specific bacteria, GCC 3, 4, 7, 10, and 14 show the presence of cells with similar morphology to those observed in extremophilic and mesophilic dissimilatory metal reducing bacteria that metabolize metal oxides (Spilde et al., 2005; El-Naggar et al., 2010; Parameswaran et al., 2013; Lusk et al., 2015a,b; 2016; 2018a; 2019a; Wang et al., 2019).

The GCC microbial community consisted of 2207 operational taxonomic units (OTUs) according to species-level annotations, representing 55 phyla. (See Table S1 for sample overview and Table S2 for taxonomy assignments of all OTUs.) As shown in Figure 5, of the 55 phyla found among all samples, the five most abundant bacterial phyla were *Actinobacteria*  $51.3 \pm 35.4\%$ , *Proteobacteria*  $12.6 \pm 9.5\%$ , *Firmicutes*  $9.8 \pm 7.3\%$ , *Bacteroidetes*  $8.3 \pm 5.9\%$ , and *Cyanobacteria*  $7.1 \pm 7.3\%$ , while the relative abundance of Archaea represented  $1.1 \pm 0.9\%$  of all samples and  $0.2 \pm 0.04\%$  of sequences were unassigned. The rarefaction curve for  $\alpha$ -diversity in 14 samples (Fig. S1) shows a slope nearing zero for all samples except GCC2, suggesting the data shown represent the true diversity of the samples with the exception of GCC2, which may have greater diversity.

Gram-positive bacteria from the phylum *Actinobacteria*, the most prevalent phylum found in GCC, have been reported to generate several bioactive compounds, produce two-thirds of all clinically used naturally-derived antibiotics, and have been indicated as likely candidates for the development of new antibiotics and antifungals (Nimaichand et al., 2012; Barka et al., 2016; Maciejewska et al., 2016; Rangseekaew and Pathom-Aree, 2019). For example, the genera *Amycolatopsis* ( $1.6 \pm 2.3\%$ ) and *Pseudonocardia* ( $16.2 \pm 17.0\%$ ) were present in all samples and previous studies have indicated that these genera may have antifungal properties (Sen et al., 2009). Furthermore, the *Streptomyces* genus, a common in-

Table 2a. Total amount in mg/L of each measured element as a function of sample number. GCC5 is not shown due to insufficient sample mass for analysis.

Sample	Digest, mg	Ag	Al	As	B	Ba	Be	Bi	Ca	Cd	Co	Cr	Cu	Fe	K	Li
GCC1	258.6	0.00	23.00	2.47	1.15	2.95	0.04	0.00	9229	0.16	0.13	1.12	0.16	414.30	9.92	0.63
GCC2	262.6	0.01	6.02	2.73	0.62	1.56	0.02	0.00	9458	0.02	0.02	0.14	0.08	217.80	3.42	0.16
GCC3	251.6	0.00	104.50	16.57	0.44	4.72	0.22	0.11	5882	0.21	0.34	5.63	1.06	2218	27.56	0.92
GCC4	250.9	0.00	0.00	2.46	0.45	5.12	0.07	0.00	9338	0.41	0.32	5.67	0.37	636.80	110.30	2.83
GCC6	264.4	0.00	0.00	0.20	0.36	2.17	0.08	0.13	182.4	0.04	0.41	2.25	0.00	2368	198.40	0.32
GCC7	260.0	0.14	0.00	15.33	0.21	39.27	0.36	0.11	1110	0.98	1.87	17.48	3.07	2663	148.50	20.71
GCC8	241.5	0.00	0.00	3.64	0.30	21.68	0.08	0.00	6734	0.08	0.49	12.24	0.28	445.80	165.50	1.15
GCC9	258.3	0.00	148.00	9.70	0.02	0.46	0.05	0.00	6570	0.04	0.11	0.49	0.31	935.60	71.32	0.15
GCC10	258.2	0.00	0.00	11.31	0.18	0.63	0.08	0.05	2813	0.04	0.45	1.08	0.52	1360	221.20	0.68
GCC11	255.2	0.00	56.13	3.20	0.07	0.31	0.03	0.00	7041	0.02	0.20	0.68	0.15	314.90	29.22	0.16
GCC12	257.1	0.00	1.58	0.16	0.00	0.16	0.00	0.00	10750	0.01	0.00	0.06	0.01	63.90	0.00	0.04
GCC13	251.1	0.00	6.62	0.70	0.00	2.22	0.01	0.00	8979	0.02	0.04	0.21	0.09	154.10	2.38	0.02
GCC14	249.8	0.00	0.00	16.16	0.50	3.77	0.11	0.00	2512	0.09	0.38	1.82	0.50	3046	218.90	0.16

Table 2b. Total amount in mg/L of each measured element as a function of sample number. GCC5 is not shown due to insufficient sample mass for analysis.

Sample	Digest, mg	Mg	Mn	Mo	Na	Ni	P	Pb	S	Sb	Se	Si	Sr	Ti	V	Zn
GCC1	258.6	7.62	131.50	0.09	5.46	0.64	25.06	2.43	0.83	0.09	0.00	5.62	0.98	1.38	1.26	6.29
GCC2	262.6	4.68	16.90	0.02	2.68	0.09	1.35	0.22	0.00	0.06	0.00	3.99	0.63	0.00	0.48	1.20
GCC3	251.6	25.25	73.18	0.34	2.51	1.71	15.43	6.56	0.82	0.14	0.17	4.61	1.91	0.00	3.43	14.31
GCC4	250.9	26.83	0.00	0.47	3.18	1.62	30.45	10.89	2.33	0.09	0.00	5.64	2.37	3.34	3.15	24.37
GCC6	264.4	40.55	6.45	0.84	21.50	0.51	37.08	1.88	1.62	0.08	0.31	5.76	1.38	0.00	4.19	1.44
GCC7	260.0	35.26	0.00	2.59	5.38	11.14	95.57	73.86	6.42	0.21	0.00	6.37	1.88	17.11	14.41	227.90
GCC8	241.5	31.87	188.50	0.72	2.43	0.93	11.39	3.44	1.80	0.13	0.41	5.31	3.15	1.73	1.79	8.72
GCC9	258.3	27.58	7.10	0.00	5.98	0.29	22.15	1.13	29.12	0.05	0.06	4.99	1.62	0.00	1.42	1.96
GCC10	258.2	63.62	27.94	0.89	7.93	1.50	79.59	1.70	51.05	0.06	0.02	4.49	1.42	0.00	1.86	4.09
GCC11	255.2	16.72	8.53	0.00	2.62	0.27	24.13	0.54	0.96	0.06	0.01	5.54	1.34	0.00	0.56	1.77
GCC12	257.1	4.26	3.31	0.00	0.29	0.02	5.70	0.02	0.00	0.03	0.00	0.45	1.88	0.09	0.07	0.30
GCC13	251.1	8.99	33.27	0.00	1.80	0.44	38.91	0.11	0.42	0.03	0.00	2.61	0.92	0.39	0.58	0.53
GCC14	249.8	32.92	66.64	0.86	2.40	1.77	98.34	3.13	1.68	0.12	0.00	5.36	0.70	0.00	3.22	2.73

habitant of limestone caves (Nimaichand et al., 2012; Také et al., 2018) and responsible for most of the commercially-available naturally-derived antibiotics on the market (Bérdy, 2005; Barka et al., 2016), composed  $2.4 \pm 3.0$  % of sequences observed across all samples. Novel *Streptomyces* species discovered in other caves located in the western United States have shown antifungal effects on *Pseudogymnoascus destructans*, a fungus that causes white-nose syndrome (WNS) in bats (Bleher et al., 2009; Hamm et al., 2017). Lastly, xerophilic members of the *Actinobacteria* phylum including the genera *Geodermatophilus* and *Modestobacter* from the *Geodermatophilaceae* family (Montero-Calasanz et al., 2012; 2013), the *Rubroacteridae* family (Bull and Asenjo, 2013), and the *Streptomyces* genus (Kurapova et al., 2012; Mohammadipanah and Wink, 2016) account for a relative abundance of  $2.7 \pm 2.8$  % across all samples observed from the cave.

*Cyanobacteria* of the family *Phormidiaceae* ( $0.5 \pm 0.7$  %) were observed in all GCC samples. They were previously observed dwelling in troglomorphic conditions within caves, including Carlsbad Cavern (Behrendt et al., 2019), and are capable of surviving for prolonged periods of time in complete darkness (Hader and Poff, 1982; Montechiaro and Giordano, 2006). Photosynthetic bacteria may be able to persist in the deep zones of the cave that harbor minimal or no surface visible light by having chlorophylls that absorb near infrared radiation (NIR) that is reflected across the limestone walls of the cave (Behrendt et al., 2019).

In addition, bacteria from the *Porphyromonadaceae* family in the phylum *Bacteroidetes* are commonly associated with acid mine drainage and sulfur reducing microbial communities (Gaidos et al., 2009; Bijmans et al., 2010) were present in nine of the 14 samples ( $0.14 \pm 0.14$  %). Finally, bacteria from the *Arcobacter* genus in the class *Epsilonproteobacteria* were observed in all samples ( $1.0 \pm 0.8$  %); previous research has indicated that these microorganisms are autotrophic and produce globular or filamentous sulfur as a metabolic end product (Wirsen et al., 2002).

Nitrogen, an essential component of amino acids and nucleotides, was found in concentrations of  $0.1 \pm 0.1$  %, and was not de-

Table 3. Total amount, in % of carbon, hydrogen, and nitrogen as a function of sample number.

Sample	Digest, mg	Carbon, %	Hydrogen, %	Nitrogen, %
GCC1	5.06	11.50	0.03	0.09
GCC2	5.03	11.89	0.00	0.05
GCC3	4.96	7.49	1.33	0.08
GCC4	5.00	8.68	0.04	0.08
GCC5	4.95	2.36	0.32	0.05
GCC6	6.63	0.25	0.35	0.05
GCC7	6.03	0.96	0.79	0.08
GCC8	5.95	9.19	0.05	0.15
GCC9	5.88	9.19	0.05	0.15
GCC10	6.25	0.59	0.58	0.05
GCC11	5.35	0.21	0.12	0.00
GCC12	5.45	0.14	0.02	0.00
GCC13	4.65	0.21	0.00	0.00
GCC14	4.44	0.34	0.09	0.00

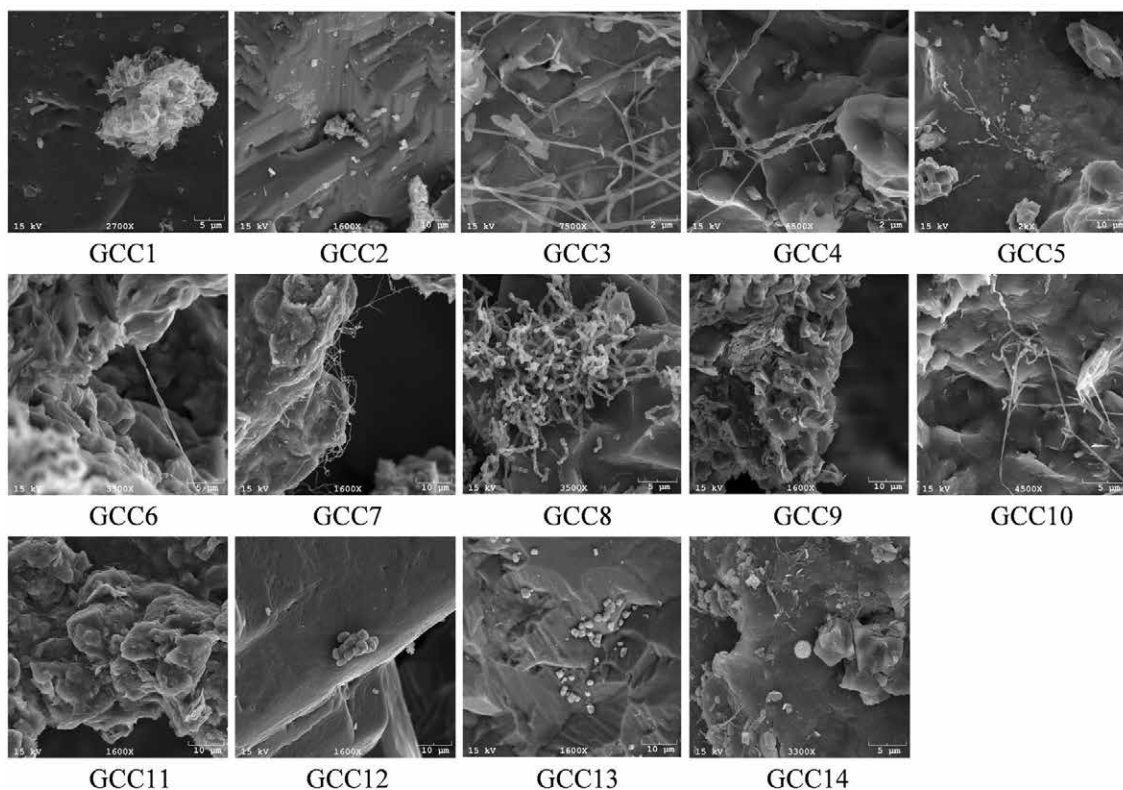


Figure 4: Scanning electron images of Samples 1-14. SEM images contain examples of multiple morphologies from diverse microorganisms. Images are at following magnifications: GCC1 2700x, GCC2 1600x, GCC3 7500x, GCC4 6500x, GCC5 2000x, GCC6 3300x, GCC7 1600x, GCC8 3500x, GCC9 1600x, GCC10 4500x, GCC11 1600x, GCC12 1600x, GCC13 1600x, GCC14 1600x.

et al., 2018) and *Burkholderiales* (Rosenblueth et al., 2018) orders suggests that nitrogen fixation may play a role in microbial communities occupying GCC (Northup et al., 2003; Wagner, 2011); however, this hypothesis requires further investigation.

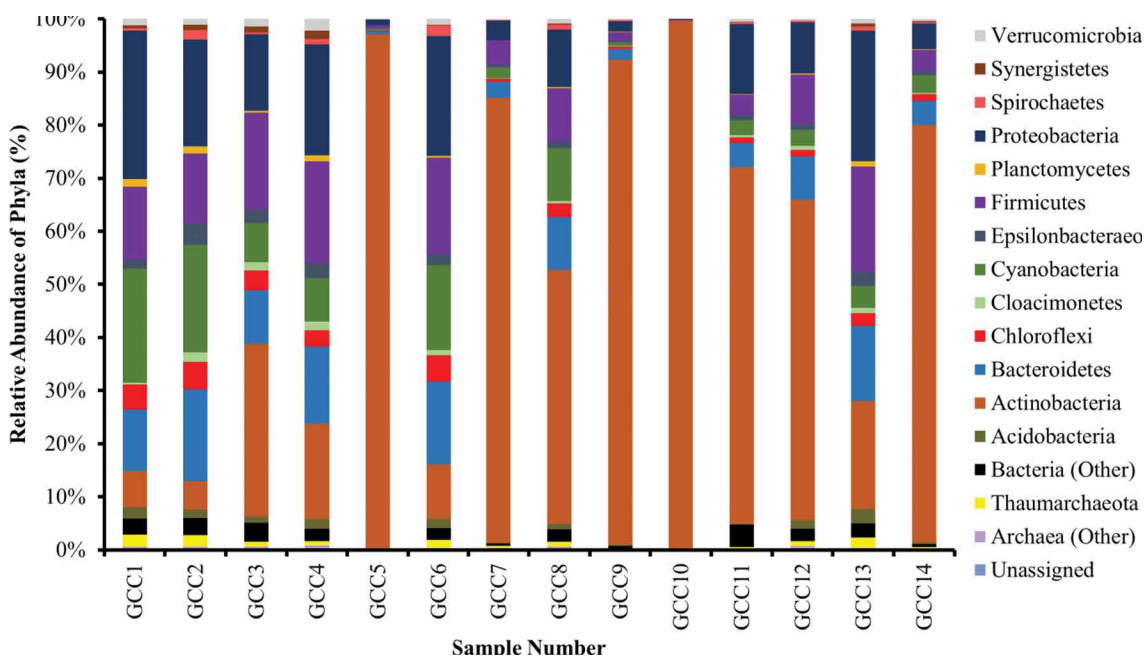


Figure 5: Relative abundance of bacterial and archaeal taxonomy at phylum level. All phyla with at least ~1% relative abundance in one or more samples are listed. Remaining phyla within the Bacteria kingdom are represented in the Bacteria (Other) category. Remaining phyla within the Archaeal kingdom are represented in the Archaea (Other) category. Unassigned sequences ( $0.2 \pm 0.04\%$ ) are also represented.

ected in samples GCC 11, 12, 13, or 14 (Table 3). This concentration of N is comparable to those observed in other caves containing nitrogen-fixing bacteria (Northup et al., 2003). The prevalence of diazotrophs ( $2.1 \pm 1.7\%$ ) including methanogenic *Euryarchaeota* (Murray and Zinder, 1984; Leigh, 2000; Bae et al., 2018), bacteria of the *Clostridium* genus (Chen et al., 2001), *Frankiaceae* from the *Actinobacteria* phylum (Santi et al., 2013), and *Rhizobiales* (Diaz-Herraiz et al., 2014; Garrido-Oter

In addition, previously characterized microorganisms that are able to reduce and oxidize materials to produce or dissolve solid metals and ores were present in all samples ( $3.8 \pm 2.9\%$ ). Observed genera include: *Geothrix* (Coates et al., 1999), *Pedomicrobium* (Northup et al., 2003), *Thiobacillus* (Provenicio et al., 2001), *Geobacter* (Bond and Lovley, 2002), *Arcobacter* (Wirsén et al., 2002), *Marinobacter* (Bo-



nis and Gralnik, 2015), *Desulfovibrio* (Payne et al., 2002), *Desulfuromonas* (Roden and Lovley 1993), *Pseudomonas* (Caspi et al., 1998), and *Shewanella* (El-Naggar et al., 2010), and the families *Desulfobulbaceae* (Pfeffer et al., 2012) and *Rhodocyclaceae* (Zhou et al., 2016). These dissimilatory metal-reducing and/or oxidizing bacteria are able to use Fe (observed in all samples at  $1141 \pm 1066$  ppm) or Mn (observed in samples GCC 1–3, 6, and 8–14 at  $43 \pm 58$  ppm) as an electron source or as a terminal electron acceptor, as shown in Equations S4–S7.

## Conclusion and Future Research

The formation of caves and karst systems relies on a complex interplay between abiotic and biotic geochemical activity (Hose et al., 2000; Kappler et al., 2005; Barton and Northup, 2007; Boston et al., 2009). In many cases, microbial communities contain the metabolic capacity to oxidize and reduce surrounding metallic ores, which greatly influences the structure and mineralogy of the cave environment (Lovley, 1993; Northup et al., 2003; Spilde et al., 2006, 2009). The microbial community data presented in this study suggests that Grand Canyon Caverns (GCC), a dry sulfuric karst cave, harbors robust extremophilic, oligotrophic, endolithic, xerotolerant, and troglomorphic microbial life within multicolored speleosol deposits found overlying its limestone walls. However, while sequencing results indicate that most of the microbial diversity within the cave speleosol has been accounted for (Fig. S1), Archaeal diversity may not be fully represented given the bias the 515f-806r bacterial/archaeal primer pair has against *Crenarchaeota/Thaumarchaeota* (Hugerth, 2014), environmental Archaea, and certain clades of Bacteria (Morris et al., 2002).

Based on the roles microbes observed in GCC play in similar caves, they are hypothesized to utilize a large repertoire of metabolic pathways including nitrogen fixation (Northup et al., 2003; Wagner, 2011), chemolithoautotrophic carbon fixation (Ramos, 2003), and dissimilatory metal reduction and oxidation (Angert et al., 1998; Povencio and Polyak, 2001; Northup et al., 2003; Macalady et al., 2006) that enables them to survive using a diverse set of electron donors and acceptors, including solid ores. Microbial reduction and oxidation of surrounding minerals and the corresponding shift in the elemental composition and oxidation states of these minerals may explain the diversity of colors observed in the cave speleosol and in the collected samples (Fig. 2 and 3). However, future studies to observe the proteomic, metagenomic, and transcriptomic profiles of the communities will offer more insight into their functional and metabolic roles.

Furthermore, finding correlations between microbial communities, surrounding cave formations, and metabolic functions may elucidate communal interactions between phyla and metabolic interactions with abiotic materials as shown in previous studies (Torres et al., 2009; Jones and Bennet, 2017). Next, a systematic study of the microbial communities collected in the cave via lab culturing will provide greater insight into the roles of these microbes in the cave ecosystem including determining the presence of carbon fixation, nitrogen fixation, or dissimilatory metal reduction/oxidation.

In addition, the cave is currently undergoing active exploration and since collecting samples for this study, new passages containing large multicolored speleosol deposits have been discovered, with a breakthrough in 2017 contributing to a ~5 % expansion in the size of the cave. The location of this discovery can be seen in Figure 1, southeast of Disappointment Dome, where the map is labelled too tight. As uncharted areas of the cave continue to be unveiled, analyzing the microbial communities inhabiting these pristine locations may lead to discoveries of novel microorganisms (Jurado et al., 2006, 2007; Bonis and Gralnik, 2015; Hamm et al., 2017) or further elucidate the role of microorganisms in the biogeochemistry of cave and karst systems (Kappler et al., 2005). The presence of microbes previously associated with the production of antifungals for WNS (Hamm et al., 2017) and the development of next generation biofuels (Bond and Lovley, 2002; Rittmann, 2008) and biotechnology (Zhou et al., 2016; Lusk et al., 2018b) also emphasizes the importance of further research to evaluate these possibilities and continued exploration of dry sulfuric cave and karst systems.

Although there are no indications of the presence of non-microbial life in the cave, future studies should investigate the presence of eukaryotic life including invertebrates, yeasts, and other fungi. In addition, human traffic in rooms where samples were collected for this study, including Sugar Hill and below the ropes to Disappointment Dome, has increased so that visitors can observe the speleosols and sampling sites. A longitudinal study can be administered to assess the impact of human activities on the cave microbiome (Leuko et al., 2017) compared to pristine areas. Future investigations may elucidate how human activity indirectly impacts the development of cave and karst systems by influencing the resident microbial communities.

## ACKNOWLEDGEMENTS

Juan Maldonado Ortiz (ASU Biological Design DNA sequencing), Misa Vening and David Lowry (SEM imaging), John McNulty (owner of Grand Canyon Caverns), Chris Laurel (Goldwater Elemental Laboratory, ASU), Paul R. Jorgenson (images in Fig. 2), Benjamin Harrold for fossil guidance, Troy Hayden for highlighting this research on the local news, the Central Arizona Grotto, the ASU Outdoors Club, and everyone who donated to Science the Earth to support the mission of Lusk 2019b to encourage democracy in the narrative of science.

## REFERENCES

- Angert, E., Northup, D., Reysenbach, A., and Peek, A., 1998, Molecular phylogenetic analysis of a bacterial community in Sulphur River, Parker Cave, Kentucky: *The American Mineralogist*, v. 83, no. 11–12, p. 1583–1592, <https://doi.org/10.2138/am-1998-1119>.
- Bae, H., Morrison, E., Chanton, J., and Ogram, A., 2018, Methanogens are major contributors to nitrogen fixation in soils of the Florida Everglades: *Applied and Environmental Microbiology*, v. 84, no. 7, p. 1–16, <https://doi.org/10.1128/AEM.02222-17>.
- Barka, E., Vatsa, P., Sanchez, L., Gaveau-Vaillant, N., Jacquard, C., Meier-Kolthoff, J., Jan P., Klenk, H., Clément, C., Ouhdouch, Y., and Van Wezel, G., 2016, Taxonomy, physiology, and Natural products of *Actinobacteria*: *Microbiology and Molecular Biology Reviews: MMBR*, v. 80, no. 1, p. 1–43, <https://doi.org/10.1128/MMBR.00019-15>.
- Barton, H., Giarrizzo, J., Suarez, P., Robertson, C., Broering, M., Banks, E., Vaishampayan, P.A., and Venkateswaran, K., 2014, Microbial diversity in a Venezuelan orthoquartzite cave is dominated by the *Chloroflexi* (Class *Ktedonobacteriales*) and *Thaumarchaeota* Group I.1c: *Frontiers in Microbiology*, v. 5, p. 615, <https://doi.org/10.3389/fmicb.2014.00615>.
- Barton, H., and Northup, D.E., 2007, Geomicrobiology in cave environments: past, current and future perspectives: *Journal of Cave and Karst Studies*, v. 69, no. 1, p. 163–178.
- Behrendt, L., Trampe, E.L., Nord, N.B., Nguyen, J., Kühn, M., Lonco, D., Nyarko, A., Dhinojwala, A., Hershey, O.S., and Barton, H., 2019, Life in the dark: Far-red absorbing cyanobacteria extend photic zones deep into terrestrial caves: *Environmental Microbiology*, v. 22, no. 3, p. 952–963, <https://doi.org/10.1111/1462-2920.14774>
- Bérdy, J., 2005, Bioactive microbial metabolites: *The Journal of Antibiotics*, v. 58, no. 1, p. 1–26.
- Bijmans, M., De Vries, E., Yang, C., N. Buisman, C., Lens, P., and Dopson, M., 2010, Sulfate reduction at pH 4.0 for treatment of process and wastewaters: *Biotechnology Progress*, v. 26, no. 4, p. 1029–1037, <https://doi.org/10.1002/btpr.400>.
- Blehert, D., Hicks, A., Behr, M., Meteyer, C., Berlowski-Zier, B., Buckles, E., Coleman, J.T.H., Darling, S.R., Gargas, A., Niver, R., Okoniewski, J.C., Rudd, R.J., and Stone, W., 2009, Bat white-nose syndrome: An emerging fungal pathogen?: *Science*, v. 323, no. 5911, p. 227, <https://doi.org/10.1126/science.1163874>.
- Bond, D., and Lovley, D., 2003, Electricity production by *Geobacter sulfurreducens* attached to electrodes: *Applied and Environmental Microbiology*, v. 69, no. 3, p. 1548–1555, <https://doi.org/10.1128/AEM.69.3.1548-1555.2003>.
- Bonis, B., and Gralnick, J., 2015, *Marinobacter subterrani*, a genetically tractable neutrophilic Fe(II)-oxidizing strain isolated from the Soudan Iron Mine: *Frontiers in Microbiology*, v. 6, p. 719, <https://doi.org/10.3389/fmicb.2015.00719>.
- Boston, P.J., Spilde, M.N., Northup, D.E., Curry, M.D., Melim, L.A., and Rosales-Lagarde, L., 2009, Microorganisms as speleogenetic agents: geochemical diversity but geomicrobial unity: *Hypogene Speleogenesis and Karst Hydrogeology of Artesian Basins*, v. 1, p. 51–58.
- Bolyen E, Rideout JR, Dillon MR, Bokulich NA, Abnet CC, Al-Ghalith GA, et al., 2019, Reproducible, interactive, scalable and extensible microbiome data science using QIIME 2: *Nature Biotechnology*, v. 37, p. 852–857, <https://doi.org/10.1038/s41587-019-0209-9>.
- Bull, A. T., and Asenjo, J. A., 2013, Microbiology of hyper-arid environments: recent insights from the Atacama Desert, Chile: *Antonie Van Leeuwenhoek*, v. 103, p. 1173–1179, <https://doi.org/10.1007/s10482-013-9911-7>.
- Caporaso, J. G., Lauber C.L., Walters, W.A., Berg-Lyons, D., Huntley, J., Fierer, N., Owens, S.M., Betley, J., Fraser, L., Bauer, M., Gormley, N., Gilbert, J.A., Smith, G., and Knight, R., 2012, Ultra-high-throughput microbial community analysis on the Illumina HiSeq and MiSeq platforms: *The ISME Journal*, v. 6, no. 8, p. 1621–1624, <https://doi.org/10.1038/ismej.2012.8>.
- Caspi, R., Tebo, B.M., and Haygood, M.G., 1998, C-Type cytochromes and manganese oxidation in *Pseudomonas putida* MnB1: *Applied and Environmental Microbiology*, v. 64, no. 10, p. 3549–3555.
- Chen, J., Toth, J., and Kasap, M., 2001, Nitrogen-fixation genes and nitrogenase activity in *Clostridium acetobutylicum* and *Clostridium beijerinckii*: *Journal of Industrial Microbiology and Biotechnology*, v. 27, no. 5, p. 281–286. <https://doi.org/10.1038/sj.jim.7000083>.
- Coates, J.D., Ellis, D.J., Gaw, C.V., and Lovley, D.R. (1999). *Geothrix fermentans* gen. nov., sp. nov., a novel Fe(III)-reducing bacterium from a hydrocarbon-contaminated aquifer: *International Journal of Systematic and Evolutionary Microbiology*, v. 49, no. 4, p. 1615–22, <https://doi.org/10.1099/00207713-49-4-1615>.
- Cunningham, K.I., Northup, D.E., Pollastro, R.M., Wright, W.G., and LaRock, E.J., 1995, Bacteria, fungi and biokarst in Lechuguilla Cave, Carlsbad Caverns National Park, New Mexico: *Environmental Geology*, v. 25, p. 2, <https://doi.org/10.1007/BF01061824>.
- Denayer, J., Poty, E., Marion, J., and Mottequin, B., 2012, Lower and Middle Famennian (Upper Devonian) rugose corals from southern Belgium and northern France: *Geologica Belgica*, v. 15, no. 4, p. 273–283.
- Dhami, N., Mukherjee, A., and Watkin, E., 2018, Microbial diversity and mineralogical-mechanical properties of calcitic cave speleothems and biomineralization conditions: *Frontiers in Microbiology*, v. 9, p. 40, <https://doi.org/10.3389/fmicb.2018.00040>.
- Diaz-Herraiz, M., Jurado, V., Cuezva, S., Laiz, L., Pallecchi, P., Tianio, P., Sanchez-Moral, S., and Saiz-Jimenez, C., 2014, Deterioration of an Etruscan tomb by bacteria from the order *Rhizobiales*: *Scientific Reports*, v. 4, no. 1, p. 3610, <https://doi.org/10.1038/srep03610>.
- Eddie, B., Wang, Z., Malanoski, A., Hall, R., Oh, S., Heiner, C., Lin, B., and Strycharz-Glaven, S., 2016, '*Candidatus tenderia electrophaga*', an uncultivated electroautotroph from a biocathode enrichment: *International Journal of Systematic and Evolutionary Microbiology*, v. 66, no. 6, p. 2178–2185, <https://doi.org/10.1099/ijsem.0.001006>.
- Edgar, R.C., Haas, B.J., Clemente, J.C., Quince, C., Knight, R., 2011, UCHIME improves sensitivity and speed of chimera detection: *Bioinformatics*, v. 27, no. 16, p. 2194–2200, <https://doi.org/10.1093/bioinformatics/btr381>.
- El-Naggar, M.Y., Wanger, G., Leung, K.M., Yuzvinsky, T.D., Southam, G., Yang, J., Lau, W.N., Neelson, K.H., and Gorby, Y.A., 2010, Electrical transport along bacterial nanowires from *Shewanella oneidensis* MR-1: *Proceedings of the National Academy of Sciences*, v. 107, no. 42, p. 18127–18131, <https://doi.org/10.1073/pnas.1004880107>.
- Emerson, D., Moyer, C., 1997, Isolation and characterization of novel iron-oxidizing bacteria that grow at circumneutral pH: *Applied and Environmental Microbiology*, v. 63, no. 12, p. 4784–4792, <https://doi.org/10.1128/AEM.63.12.4784-4792.1997>.
- Engel, A., Stern, L., Bennett, P., 2004, Microbial contributions to cave formation: New insights into sulfuric acid speleogenesis: *Geology*, v. 32, no. 5, p. 369–372, <https://doi.org/10.1130/G20288.1>.
- Forbes, J., 1998, Air temperature and relative humidity study: Torgac Cave, New Mexico: *Journal of Cave and Karst Studies*, v. 60, no. 1, p. 27–32.
- Erlich, H.L., 1980, Different forms of microbial manganese oxidation and reduction and their environmental significance: *in* Trudinger, P.A., Walter, M.R., Ralph, B.J., eds., *Biogeochemistry of Ancient and Modern Environments*. Springer, Berlin, Heidelberg, p. 327–332.
- Gaidos, E., Marteinson, V., Thorsteinsson, T., Jóhannesson, T., Rúnarsson, A.R., Stefansson, A., Glazer, B., Lanoil, B., Skidmore, M., Han, S., Miller, M., Rusch, A., and Foo, W., 2008, An oligarchic microbial assemblage in the anoxic bottom waters of a volcanic subglacial lake: *The ISME Journal*, v. 3, no. 4, p. 486–497, <https://doi.org/10.1038/ismej.2008.124>.

- Gao, L., Lu, X., Liu, H., Li, J., Li, W., Song, R., Wang, R., Zhang, D., and Zhu, J., 2019, Mediation of extracellular polymeric substances in microbial reduction of hematite by *Shewanella oneidensis* MR-1: *Frontiers in Microbiology*, v. 10, no. 575, p. 1–12, <https://doi.org/10.3389/fmicb.2019.00575>
- Garrido-Oter, R., Nakano, R.T., Dombrowski, N., Ma, K., Mchardy, A.C., and Schulze-Lefert, P., 2018, Modular traits of the *Rhizobiales* root microbiota and their evolutionary relationship with symbiotic *Rhizobia*: *Cell Host & Microbe*, v. 24, no. 1, p. 155–167.e5, <https://doi.org/10.1016/j.chom.2018.06.006>
- Gootee, B.F., 2014, The Redwall Limestone – The fascinating history and character of Grand Canyon's thickest limestone: PowerPoint presentation, Grand Canyon guide training seminar 8 February 2014, 1–27, Accessed online: [http://repository.azgs.gov/sites/default/files/dlio/files/nid1572/gootee\\_redwall\\_limestone\\_gts\\_2014.pdf](http://repository.azgs.gov/sites/default/files/dlio/files/nid1572/gootee_redwall_limestone_gts_2014.pdf)
- Gootee, B.F., 2019, Geological timeframe of the Grand Canyon: Arizona Geological Survey Open-File Report ORF-19-02, p. 1–2.
- Hader, D., and Poff, K.L., 1982, Dependence of the photophobic response of the blue-green alga, *Phormidium uncinatum*, on cations: *Archives of Microbiology*, v. 132, p. 345–348, <https://doi.org/10.1007/BF00413387>
- Hamm, P., Caimi, N., Northup, D., Valdez, E., Buecher, D., Dunlap, C., Labeda, D.P., Lueschow, S., and Porras-Alfaro, A., 2017, Western bats as a reservoir of novel *Streptomyces* species with antifungal activity: *Applied and Environmental Microbiology*, v. 83, no. 5, p. 1–10, <https://doi.org/10.1128/AEM.03057-16>
- Hill, C.A., 1987, Geology of Carlsbad Cavern and other caves in the Guadalupe Mountains, New Mexico and Texas, Socorro: New Mexico Bureau of Mines and Mineral Resources, Bulletin 117.
- Hose, L.D., Palmer, A.N., Palmer, M.V., Northup, D.E., Boston, P.J., and Duchene, H.R., 2000, Microbiology and geochemistry in a hydrogen-sulfide-rich karst environment: *Chemical Geology*, v. 169, no. 3–4, p. 399–423, [https://doi.org/10.1016/S0009-2541\(00\)00217-5](https://doi.org/10.1016/S0009-2541(00)00217-5)
- Huddle, J.W., and Dobrovolsky, E., 1952, Devonian and Mississippian rocks of central Arizona: Shorter Contributions to General Geology, Geological Survey Professional Paper 233-D. <https://pubs.usgs.gov/pp/0233d/report.pdf>Hugert L.W., Wefer H.A., Lundin S., Jakobsson H.E., Lindberg M., Rodin S., Engstrand L., Andersson A.F., 2014, DegePrime, a program for degenerate primer design for broad-taxonomic-range PCR in microbial ecology studies: *Applied and Environmental Microbiology*, v. 80, p. 5116–5123. <https://doi.org/10.1128/AEM.01403-14>
- Jones, A., and Bennett, P., 2017, Mineral Ecology: Surface Specific Colonization and Geochemical Drivers of Biofilm Accumulation, Composition, and Phylogeny: *Frontiers in Microbiology*, v. 8, no. 491, p. 1–14, <https://doi.org/10.3389/fmicb.2017.00491>
- Jurado, V., Gonzalez, J., Laiz, L., and Saiz-Jimenez, C., 2006, *Aurantimonas altamirensis* sp. nov., a member of the order *Rhizobiales* isolated from Altamira Cave: *International Journal of Systematic and Evolutionary Microbiology*, v. 56, no. 11, p. 2583–2585, <https://doi.org/10.1099/ijs.0.64397-0>
- Jurado, V., Laiz, L., Gonzalez, J.M., and Saiz-Jimenez, C., 2007, Cave research: understanding biodiversity through conservation studies: *Coalition*, v. 13, no. 3, p. 4–6.
- Kappler, A., Emerson, D., Edwards, K., Amend, J., Gralnick, J., Grathwohl, P., Hoehler, T., and Straub, K., 2005, Microbial activity in biogeochemical gradients – new aspects of research: *Geobiology*, v. 3, no. 3, p. 229–233, <https://doi.org/10.1111/j.1472-4669.2005.00053.x>
- Klimchouk, A.B., Ford, D.C., Palmer, A., Wolfgang, D., 2000, Speleogenesis: Evolution of karst aquifers: *Journal of Hydrology*, ed. Jan 2000, p. 244–260, [https://doi.org/10.1016/S0022-1694\(00\)00341-3](https://doi.org/10.1016/S0022-1694(00)00341-3)
- Kurapova, I., Zenova, G. M., Sudnitsyn, I. I., Kizilova, A. K., Manucharova, N. A., Norovsuren, Z. H., and Zvyagontsev, D.G., 2012, Thermotolerant and thermophilic *Actinomycetes* from soils of Mongolia Desert Steppe Zone: *Microbiology*, v. 81, p. 98–108, <https://doi.org/10.1134/S0026261712010092>
- Laetsch, T., Downs, R. T., 2006, Software for the identification and refinement of cell parameters from powder diffraction data of minerals using the RRUFF project and American Mineralogist Crystal Structure Databases: Abstracts from the 19<sup>th</sup> general meeting of the International Mineralogical Association, Kobe, Japan, 23–28 July 2006. Accessed online: [https://www.geo.arizona.edu/xtal/group/pdf/IMA19\\_P08-25.pdf](https://www.geo.arizona.edu/xtal/group/pdf/IMA19_P08-25.pdf)
- Lebre, P., De Maayer, P., Cowan, D., 2017, Xerotolerant bacteria: surviving through a dry spell: *Nature Reviews Microbiology*, v. 15, p. 285–296, <https://doi.org/10.1038/nrmicro.2017.16>
- Leuko, S., Koskinen, K., Sanna, L., Paolo, M., Moissl-Eichinger, C., and Rettberg, P., 2017, The influence of human exploration on the microbial community structure and ammonia oxidizing potential of the Su Bentu limestone cave in Sardinia, Italy: *PLoS One*, v. 12, no. 7, p. E0180700, <https://doi.org/10.1371/journal.pone.0180700>
- Leigh, J.A., 2000, Nitrogen fixation in methanogens: the archaeal perspective: *Current Issues in Molecular Biology*, v. 2, no. 4, p. 125–131.
- Lovley, D., 1993, Dissimilatory metal reduction: *Annual Review of Microbiology*, v. 47, no. 1, p. 263–290, <https://doi.org/10.1146/annurev.mi.47.100193.001403>
- Lusk, B.G., 2019a, Thermophiles; or, the modern Prometheus: the importance of extreme microorganisms for understanding and applying extracellular electron transfer: *Frontiers in Microbiology*, v. 10, p. 818, <https://doi.org/10.3389/fmicb.2019.00818>
- Lusk, B.G., 2019b, The importance of the democratic and multidirectional exchange of values between scientists, STEM educators, and historically underrepresented members of the community: *Journal of Responsible Innovation*, v. 6, no. 2, p. 248–254, <https://doi.org/10.1080/23299460.2019.1571894>
- Lusk, B.G., Badalamenti, J., Parameswaran, P., Bond, D., and Torres, C., 2015a, Draft genome sequence of the Gram-positive thermophilic iron reducer *Thermincola ferriacetica* strain Z-0001T: *Genome Announcements*, v. 3, no. 5, p. 1–2, <https://doi.org/10.1128/genomeA.01072-15>
- Lusk, B.G., Colin, A., Parameswaran, P., Rittmann, B., and Torres, C., 2018a, Simultaneous fermentation of cellulose and current production with an enriched mixed culture of thermophilic bacteria in a microbial electrolysis cell: *Microbial Biotechnology*, v. 11, no. 1, p. 63–73, <https://doi.org/10.1111/1751-7915.12733>
- Lusk, B.G., Khan, Q., Parameswaran, P., Hameed, A., Ali, N., Rittmann, B., and Torres, C., 2015b, Characterization of electrical current-generation capabilities from thermophilic bacterium *Thermoanaerobacter pseudethanolicus* using xylose, glucose, cellobiose, or acetate with fixed anode potentials: *Environmental Science & Technology*, v. 49, no. 24, p. 14725–14731, <https://doi.org/10.1021/acs.est.5b04036>
- Lusk, B.G., Parameswaran, P., Papat, S.C., Rittmann, B.E., and Torres, C.I., 2016, The effect of pH and buffer concentration on anode biofilms of *Thermincola ferriacetica*, *Bioelectrochemistry*, v. 112, p. 47–52, <https://doi.org/10.1016/j.bioelechem.2016.07.007>
- Lusk, B.G., Zhou, C., Tomaswick, A., and Rittmann, B.E., 2018b, Using the membrane biofilm reactor (MBfR) to recover platinum group metals (PGMs) as nanoparticles from wastewater: *TechConnect Briefs*, v. 2, p. 134–137, ISBN 978-0-9988782-3-2.
- Macalady, J.L., Lyon, E.H., Koffman, B., Albertson, L.K., Meyer, K., Galdenzi, S., and Mariani, S., 2006, Dominant microbial populations in limestone-corroding stream biofilms, Frasassi Cave System, Italy: *Applied and Environmental Microbiology*, v. 72, no. 8, p. 5596–5609, <https://doi.org/10.1128/AEM.00715-06>
- Maciejewska, M., Adam, D., Martinet, L., Naomé, A., Calusinska, M., Smargiasso, N., Paw, E.D., Barton, H., Carnol, M., Hanikenne, M., Hayette, M., Delposse, P., Baurain, D., Rigali, S., 2016, A phenotypic and genotypic analysis of the antimicrobial potential of cultivable *Streptomyces* isolated from cave moonmilk deposits: *Frontiers in Microbiology*, v. 7, p. 1–19, <https://doi.org/10.3389/fmicb.2016.01455>

- Mohammadipanah, F., and Wink, J., 2015, *Actinobacteria* from arid and desert habitats: diversity and biological activity: *Frontiers in Microbiology*, v. 6, p. 1541, <https://doi.org/10.3389/fmicb.2015.01541>.
- Montero-Calasanz, M., Göker, M., Pötter, G., Rohde, M., Spröer, C., Schumann, P., Gorbushina A.A., Klenk H.P., 2012, *Geodermatophilus arenarius* sp. nov., a xerophilic actinomycete isolated from Saharan desert sand in Chad: *Extremophiles*, v. 16, p. 903–909, <https://doi.org/10.1007/s00792-012-0486-4>.
- Montero-Calasanz, M. C., Göker, M., Pötter, G., Rohde, M., Spröer, C., Schumann, P., Gorbushina A.A., Klenk H.P., 2013, *Geodermatophilus siccatatus* sp. nov., isolated from arid sand of the Saharan desert in Chad: *Antonie Van Leeuwenhoek*, v. 103, p. 449–456, <https://doi.org/10.1007/s10482-012-9824-x>.
- Montechiaro, F., and Giordano, M., 2006, Effect of prolonged dark incubation on pigments and photosynthesis of the cave-dwelling cyanobacterium *Phormidium autumnale* (*Oscillatoriales*, *Cyanobacteria*): *Phycologia*, v. 45, no. 6, p. 704–710, <https://doi.org/10.2216/06-15.1>.
- Morris R.M., Rappé M.S., Connon S.A., Vergin K.L., Siebold W.A., Carlson C.A., Giovannoni S.J., 2002, SAR11 clade dominates ocean surface bacterioplankton communities: *Nature*, v. 420, p. 806–810, <https://doi.org/10.1038/nature01240>.
- Nimaichand, S., Zhu, W., Yang, L., Ming, H., Nie, G., Tang, S., Ningthoujam, D., and Li, W., 2012, *Streptomyces manipurensis* sp. nov., a novel actinomycete isolated from a limestone deposit site in Manipur, India: *Antonie Van Leeuwenhoek*, v. 102, no. 1, p. 133–139, <https://doi.org/10.1007/s10482-012-9720-4>.
- Northup, D., Barns, S., Yu, L., Spilde, M., Schelble, R., Dano, K., Crossey, L.J., Connolly, C.A., Boston, P.J., Natvig, D.O., and Dahm, C., 2003, Diverse microbial communities inhabiting ferromanganese deposits in Lechuguilla and Spider Caves: *Environmental Microbiology*, v. 5, no. 11, p. 1071–1086, <https://doi.org/10.1046/j.1462-2920.2003.00500.x>.
- Northup, D. E., Melim, L.A., Spilde, M.N., Hathaway, J.M., Garcia, M.G., Moya, M., Stone, F.D., Boston, P.J., Dapkevicius, M.E.N.L., Riquelme, C., 2011, Lava cave microbial communities within mats and secondary mineral deposits: Implications for life detection on other planets: *Astrobiology*, v. 11, no. 7, p. 601–618, <https://doi.org/10.1089/153110701750137413>.
- Parameswaran, P., Bry, T., Popat, S., Lusk, B., Rittmann, B., and Torres, C., 2013, Kinetic, electrochemical, and microscopic characterization of the thermophilic, anode-respiring bacterium *Thermincola ferriacetica*: *Environmental Science & Technology*, v. 47, no. 9, p. 4934–4940, <https://doi.org/10.1021/es400321c>.
- Pedregosa, F., Varoquaux, G., Gramfort, A., Michel, V., Thirion, B., Grisel, O., Blondel, M., Müller, A., Nothman, J., Louppe, G., Prettenhofer, P., Weiss, R., Dubourg, V., Vanderplas, J., Passos, A., Cournapeau, D., Brucher, M., Perrot, M., Duchesnay, E., 2018, Scikit-learn: Machine Learning in Python: *Journal of Machine Learning Research*, arXiv:1201.0490v4 [cs.LG].
- Murray, P.M. and Zinder, S.H., 1984, Nitrogen fixation by a methanogenic archaeobacterium: *Nature*, v. 312, no. 5991, p. 284–286, <https://doi.org/10.1038/312284a0>.
- Myers, C., and Neelson, K., 1988, Bacterial manganese reduction and growth with manganese oxide as the sole electron acceptor: *Science*, v. 240, no. 4857, p. 1319–1321, <https://doi.org/10.1126/science.240.4857.1319>.
- Payne, R.B., Gentry, D.M., Rapp-Giles, B.J., Casalot, L., and Wall, J.D., 2002, Uranium reduction by *Desulfovibrio desulfuricans* strain G20 and a cytochrome c3 mutant: *Applied and Environmental Microbiology*, v. 68, no. 6, p. 3129–3132, <https://doi.org/10.1128/aem.68.6.3129-3132.2002>.
- Pedder, A., and Murphy, M., 2004, Emsian (Lower Devonian) rugosa of Nevada: revision Of systematics and stratigraphic ranges, and reassessment of faunal provincialism: *Journal of Paleontology*, v. 78, no. 5, p. 838–865, [https://doi.org/10.1666/0022-3360\(2004\)078<0838:ELDRON>2.0.CO;2](https://doi.org/10.1666/0022-3360(2004)078<0838:ELDRON>2.0.CO;2).
- Pfeffer, C., Larsen, S., Song, J., Dong, M., Basenbacher, F., Meyer, R.L., Kjekdsen, K.U., Schreiber, L., Gorby, Y.A., El-Naggar, M.Y., Leung, K.M., Schramm, A., Risgaard-Petersen, N., and Nielsen, L.P., 2012, Filamentous bacteria transport electrons over centimetre distances: *Nature*, v. 491, no. 7423, p. 218–221, <https://doi.org/10.1038/nature11586>.
- Price, L.G., 1999, Geology of the Grand Canyon. Grand Canyon, Arizona: Grand Canyon Association, 64 p.
- Provencio, P., Victor J., and Polyak, P., 2001, Iron oxide-rich filaments: possible fossil bacteria in Lechuguilla Cave, New Mexico: *Geomicrobiology Journal*, v. 18, no. 3, p. 297–309, <https://doi.org/10.1080/01490450152467804>.
- Quast, C., Pruesse, E., Yilmaz, P., Gerken, J., Schweer, T., Yarza, P., Peplies, G., Glöckner, F., 2013, The SILVA ribosomal RNA gene database project: Improved data processing and web-based tools: *Nucleic Acids Research*, v. 41, no. D1, D590–D596, <https://doi.org/10.1093/nar/gks1219>.
- Ramos, J.L., 2003, Lessons from the genome of a lithoautotroph: making biomass from almost nothing: *Journal of Bacteriology*, v. 185, no. 9, p. 2690–2691, <https://doi.org/10.1128/jb.185.9.2690-2691.2003>.
- Rangseekaew, P., and Pathom-Aree, W., 2019, Cave *Actinobacteria* as producers of bioactive metabolites: *Frontiers in Microbiology*, v. 10, p. 387, <https://doi.org/10.3389/fmicb.2019.00387>.
- Rideout, J., He, Y., Navas-Molina, J., Walters, W., Ursell, L., Gibbons, S., Chase, J., McDonald, D., Gonzalez, A., Robbins-Pianka, A., Clemente, J., Gilbert, J., Huse, S., Zhou, H., Knight, R., Caporaso, J., and Argonne National Lab, 2014, Subsampled open-reference clustering creates consistent, comprehensive OTU definitions and scales to billions of sequences: *PeerJ* 2, no. E545, <https://doi.org/10.7717/peerj.545>.
- Rittmann, B., 2008, Opportunities for renewable bioenergy using microorganisms: *Biotechnology and Bioengineering*, v. 100, no. 2, p. 203–212, <https://doi.org/10.1002/bit.21875>.
- Roden, E., Lovley, D., 1993, Dissimilatory Fe(III) reduction by the marine microorganism *Desulfuromonas acetoxidans*: *Applied and Environmental Microbiology*, v. 59, no. 3, p. 734–742, <https://doi.org/10.1128/AEM.59.3.734-742.1993>.
- Rosenblueth, M., Ormeño-Orrillo, E., López-López, A., Rogel, M.A., Reyes-Hernández, B.J., Martínez-Romero, J.C., Reddy, P.M., and Martínez-Romero, E., 2018, Nitrogen fixation in cereals: *Frontiers in Microbiology*, v. 9, p. 1794, <https://doi.org/10.3389/fmicb.2018.01794>.
- Santi, C., Bogusz, D., and Franche, C., 2013, Biological nitrogen fixation in non-legume plants: *Annals of Botany*, v. 111, no. 5, p. 743–767, <https://doi.org/10.1093/aob/mct048>.
- Sen, R., Ishak, H.D., Estrada, D., Dowd, S.E., Hong, E., and Mueller, U.G., 2009, Generalized antifungal activity and 454-screening of *Pseudonocardia* and *Amycolatopsis* bacteria in nests of fungus-growing ants: *Proceedings of the National Academies of Sciences*, v. 106, no. 42, p. 17805–17810, <https://doi.org/10.1073/pnas.0904827106>.
- Snoeyink, V.L., and Jenkins, D., 1980, *Water Chemistry*. John Wiley & Sons, p. 380-381, ISBN 0-471-05196-9.
- Spilde, M.N., Kooser, A., Boston, P.J., and Northup, D.E., 2009, Speleosol: a subterranean soil: *Minerology*, *Proceedings of the 15<sup>th</sup> International Conference of Speleology*, p. 338–334.
- Spilde, M.N., Northup, D.E., Boston, P.J., Schelble, R.T., Dano, K.E., Crossey, L.J., 2005, Geomicrobiology of cave ferromanganese deposits: a field and laboratory investigation: *Geomicrobiology Journal*, v. 22, p. 99–116, <https://doi.org/10.1080/0149045090945889>.

- Spilde, M.N., Northup, D.E., Boston, P.J., 2006, Ferromanganese deposits in the caves of the Guadalupe Mountains: New Mexico Geological Society guidebook, 57<sup>th</sup> conference, Caves and Karst of Southeast New Mexico, p. 161–166.
- Sun, Y., Tang, H., Ribbe, A., Duzhko, V., Woodard, T., Ward, J., Joy, E., Bai, Y., Nevin, K.P., Nonnenmann, S.S., Russell, T., Emrick, T., and Lovley, D., 2018, Conductive composite materials fabricated from microbially produced protein nanowires: *Small*, v. 14, no. 44, p. 1–5, <https://doi.org/10.1002/sml.201802624>.
- Také, A., Inahashi, Y., Ômura, S., Takahashi, Y., & Matsumoto, A., 2018, *Streptomyces boninensis* sp. nov., isolated from soil from a limestone cave in the Ogasawara Islands: *International Journal of Systematic and Evolutionary Microbiology*, v. 68, no. 5, p. 1795–1799. <https://doi.org/10.1099/ijsem.0.002753>.
- Tisato, N., Torriani, S.F.F., Monteux, S., Sauro, F., Waele, J.D., Tavagna, M.L., D'Angeli, I.M., Chailloux, D., Renda, M., Eglinton, T.I., and Bonognali, T.R.R., 2015, Microbial mediation of complex subterranean mineral structures: *Scientific Reports*, v. 5, no. 1, p. 15525, <https://doi.org/10.1038/srep15525>.
- Torres, C., Krajmalnik-Brown, R., Parameswaran, P., Marucs, A., Wanger, G., Gorby, Y., Rittmann, B., 2009, Selecting Anode-Respiring Bacteria Based on Anode Potential: Phylogenetic, Electrochemical, and Microscopic Characterization: *Environmental Science and Technology*, v. 43, p. 9519–9524, <https://doi.org/10.1021/es902165y>.
- Wagner, S. C., 2011, Biological nitrogen fixation: *Nature Education Knowledge*, v. 3, no. 10, p. 15.
- Wang, F., Gu, Y., O'Brien, J.P., Yi, S.M., Yalcin, S.E., Srikanth, V., Shen, C., Vu, D., Ing, N.L., Hochbaum, A.I., Egelman, E.H., and Malvankar, N.S., 2019, Structure of microbial nanowires reveals stacked hemes that transport electrons over micrometers: *Cell*, v. 177, no. 2, p. 361–369. e10, <https://doi.org/10.1016/j.cell.2019.03.029>.
- Wang, X., Schröder, H.C., Wiens, M., Schloßmacher, U., and Müller, W.E.G., 2009, Manganese/polymetallic nodules: micro-structural characterization of exolithobiontic- and endolithobiontic microbial biofilms by scanning electron microscopy: *Micron*, v. 40, no. 3, p. 350–358, <https://doi.org/10.1016/j.micron.2008.10.005>.
- Weber, K.A., Achenbach, L.A., and Coates, J.D., 2006, Microorganisms pumping iron: anaerobic microbial iron oxidation and reduction: *Nature Reviews Microbiology*, v. 4, no. 10, p. 752–764, <https://doi.org/10.1038/nrmicro1490>.
- Wierzchos, J., Cámara, B., De Los Ríos, A., Davila, A.F., Sánchez Almazo, I.M., Artieda, O., Wierzchos, K., Gomez-Silva, B., Mckay, C., and Ascaso, C., 2011, Microbial colonization of Ca-sulfate crusts in the hyperarid core of the Atacama Desert: implications for the search for life on Mars: *Geobiology*, v. 9, no. 1, p. 44–60, <https://doi.org/10.1111/j.1472-4669.2010.00254.x>.
- Wirsen, C. O., Sievert, S. M., Cavanaugh, C. M., Molyneaux, S. J., Ahmad, A., Taylor, L. T., Delong, E.F., and Taylor, C. D., 2002, Characterization of an autotrophic sulfide-oxidizing marine *Arcobacter* sp. that produces filamentous sulfur: *Applied and Environmental Microbiology*, v. 68, no. 1, p. 316–325, <https://doi.org/10.1128/aem.68.1.316-325.2002>.
- Zhang, F., Lin, C., Bian, L., Glasby, G.P., and Zhamoïda, V.A., 2002, Possible evidence for the biogenic formation of spheroidal ferromanganese concretions from the eastern Gulf of Finland, the Baltic Sea: *Baltica*, v. 15, p. 23–29.
- Zhou, C., Ontiveros-Valencia, A., Wang, Z., Maldonado, J., Zhao, H., Krajmalnik-Brown, R., and Rittmann, B., 2016, Palladium recovery in a H<sub>2</sub>-based membrane biofilm reactor: formation of Pd(0) nanoparticles through enzymatic and autocatalytic reductions: *Environmental Science & Technology*, v. 50, no. 5, p. 2546–2555, <https://doi.org/10.1021/acs.est.5b05318>.